

1 Influence of mussel culture on the vertical export of phytoplankton  
2 carbon in a coastal upwelling embayment (Ría de Vigo, NW Iberia)

3

4 M. Froján<sup>a,\*</sup>, F.G. Figueiras<sup>a</sup>, D. Zúñiga<sup>b, c</sup>, F. Alonso-Pérez<sup>a</sup>, B. Arbones<sup>a</sup>, C.G. Castro<sup>a</sup>

5

6 <sup>a</sup>Instituto de Investigacións Mariñas (IIM) CSIC, E-36208, Vigo, Spain

7 <sup>b</sup>Instituto Português do Mar e da Atmosfera (IPMA), Div. Geologia e Georecursos

8 Marinhos, 1749-077, Lisbon, Portugal

9 <sup>c</sup>Universidad de Vigo, Departamento de Física Aplicada, Campus Lagoas-Marcosende,

10 E-36310, Vigo, Spain

11

12

13

14

15

16

17

18

19 \*Corresponding author:

20 E-mail address: [mariafrojan@iim.csic.es](mailto:mariafrojan@iim.csic.es)

21 Phone: +34986231930

22 Fax: +34986292762

23

24

25 ABSTRACT

26 The goal of this paper is to find out whether suspended mussel culture affects the  
27 vertical fluxes of biogenic particles in the Ría de Vigo on a seasonal scale. With this  
28 aim, vertical fluxes of particulate organic carbon (POC), and the magnitude and  
29 composition of vertical export of phytoplankton carbon (C<sub>phyto</sub>) collected in sediment  
30 traps, were examined by comparing data obtained inside a mussel farming area (RaS),  
31 with those found at a reference station (ReS) not affected by mussels. Our results  
32 indicate that mussel farming has a strong impact on sedimentation fluxes under the  
33 rafts, not only increasing POC flux, but also altering the magnitude and composition of  
34 C<sub>phyto</sub> fluxes. Average POC flux at RaS ( $2564 \pm 1936 \text{ mg m}^{-2} \text{ d}^{-1}$ ) was 4 times higher  
35 than at ReS ( $731 \pm 276 \text{ mg m}^{-2} \text{ d}^{-1}$ ), and much of this increase was due to biodeposit  
36 fluxes (C<sub>biodep</sub>) which accounted for large proportion of POC flux (35–60%). Indeed,  
37 because of this high C<sub>biodep</sub> flux, only a small proportion of the POC flux was due to  
38 C<sub>phyto</sub> flux (3–12 %). At the same time, we observed an increased sedimentation of  
39 phytoplankton cells at RaS that could be explained by a combination of mechanisms:  
40 less energetic hydrodynamic conditions under mussel rafts, ballast effect by sinking  
41 mussel feces and diatoms aggregates. Moreover, mussel farming also altered the quality  
42 of the C<sub>phyto</sub> flux by removing part of the predatory pressure of zooplankton, and thus  
43 matching diatom composition in water column and sediment traps.

44

45

46

47

48 Keywords: Phytoplankton, Mussel culture, Sedimentation flux, Biodeposits,  
49 Upwelling, Ría de Vigo

## 50 1. INTRODUCTION

51 Mussels are filter-feeders that clear large amounts of phytoplankton and other  
52 organic and inorganic particles suspended in the water column, repacking them into  
53 rapidly sinking fecal pellets (Jaramillo et al. 1992). This feeding behavior enhances the  
54 sedimentation in farming areas (Dahbläck and Gunnarsson 1981), diverting primary  
55 production and energy flow from planktonic to benthic food webs (Dame 1996;  
56 Cranford et al. 2003) and potentially enriching the underlying sediments with organic  
57 matter (Callier et al. 2006; Giles et al. 2006; Cranford et al. 2009). Quantifying this  
58 sedimentation flux and knowing its plankton composition is necessary to improve our  
59 management of coastal areas with significant mussel farming activity.

60 The Rías Baixas are four coastal embayments located on the NW Iberia (Fig. 1),  
61 where mussel is cultured on intensive scale (Tenore et al. 1982; Blanton et al. 1987;  
62 Figueiras et al. 2002). For these coastal inlets influenced by upwelling, it has been  
63 observed a strong connection between size structure and metabolic balance of the  
64 microbial plankton community, so that the autotrophy degree of the Rías was higher  
65 with greater contribution of larger phytoplankton (Cermeño et al. 2006; Arbones et al.  
66 2008). The dominance of microplankton ( $> 20 \mu\text{m}$ ), especially diatoms, for much part  
67 of the year is associated with high values of net community production (NCP), which  
68 implies a high export capacity of biogenic carbon outside the microbial community  
69 (Tremblay and Legendre 1994; Smith and Kemp 1995; Buesseler 1998). But under  
70 mussel rafts, the lower irradiance that cause the decrease in gross primary production  
71 (GPP), and the consumption of large sizes of microbial plankton by mussels (Froján et  
72 al. 2014) has been related with the decrease in NCP in the raft area (Froján et al.  
73 submitted). This ability of mussel culture to affect primary production and metabolic  
74 balance of the microbial community would presumably result in a reduction in the

75 export capacity of the microbial plankton community as a consequence of mussel  
76 farming.

77 To date, most studies about sedimentation of organic matter in the NW Iberian  
78 upwelling region (Bode et al. 1998; Olli et al. 2001; Varela et al. 2004; Alonso-Pérez et  
79 al. 2010) focused on the magnitude of vertical fluxes of particulate organic carbon  
80 (POC). Recently, Zúñiga et al. (2011) showed that phytoplankton carbon flux ( $C_{\text{phyto}}$ )  
81 accounted for up to 49 % of total POC flux in the Ría de Vigo during the summer  
82 upwelling, supporting the hypothesis that sedimentation of phytoplankton living cells  
83 may become an important component of POC flux (Fowler and Knauer 1986; Turner  
84 2015). The few available studies about sedimentation under mussel rafts in the Galician  
85 Rías showed vertical fluxes of POC significantly higher than those outside the mussel  
86 influence zone (Cabanias et al. 1979; Tenore et al. 1982; Alonso-Pérez et al. 2010;  
87 Zúñiga et al. 2014). Moreover, Zúñiga et al. (2014) found a strong relationship between  
88 seasonal variability in biodeposition of mussels and variability in sedimentation rates  
89 under the rafts in the Ría de Ares-Betanzos. However, mussel culture influence on  
90 phytoplankton sedimentation in the Rías remains unknown. At this stage, the working  
91 hypothesis is that mussel farming may alter the natural sedimentation rates at the raft  
92 area, not only by increasing POC flux by mussel biodeposition, but also by reducing  
93  $C_{\text{phyto}}$  flux due to mussel grazing.

94 In this regard, our study aims to evaluate for the first time how mussel culture  
95 influences the quality of POC fluxes in the Ría de Vigo. To this end, we examined the  
96 magnitude and composition of  $C_{\text{phyto}}$  fluxes collected in sediment traps, in relation to  
97 the quantity and quality of the phytoplankton community in the water column. The  
98 results from this study provide new information about the role played by mussel culture  
99 on the carbon cycle in this coastal upwelling region.

## 100 2. MATERIALS AND METHODS

### 101 2.1. Characterization of the water column and vertical export

102 In the framework of the Spanish project RAFTING (Impact of mussel raft culture on  
103 the benthic-pelagic coupling in a Galician Ría), 24 oceanographic cruises were carried  
104 out between 2007 and 2008, covering the four seasonal periods characteristic of the  
105 region, autumn (September 17 to October 4), winter (January 28 to February 14), spring  
106 (April 14 to May 01) and summer (June 26 to July 14). During these sampling periods,  
107 **daily water column observations were carried out on board R/V ‘Mytilus’ at 2 stations**  
108 in the Ría de Vigo (Fig. 1): a reference station (ReS) and a raft station (RaS). The ReS  
109 was positioned in the central channel of the Ría (42 m maximum depth), well outside of  
110 the mussel farming area, a position that has been well-established as a reference site for  
111 studies concerning short-term and seasonal variability in the Ría de Vigo (e.g. Nogueira  
112 et al. 2000; Nogueira and Figueiras 2005; Crespo et al. 2006). The RaS was located  
113 slightly inwards in the Ría, within a raft polygon (group of rafts). Mussel rafts have an  
114 area of 500 m<sup>2</sup> which are 100 m apart and from its wooden structure hang a maximum  
115 of 500 ropes 12 m long with mussels attached. Under these conditions, mussels grow  
116 fast and are able to reach the commercial size (70 to 95 mm) within a relatively short  
117 period of time (16–18 months; Pérez-Camacho et al. 2013). At both sampling stations  
118 water samples were collected at nominal depths (surface, 5, 10, 15 and 20 m), using a  
119 CTD SBE 9/11 (SeaBird) fitted to an oceanographic rosette equipped with 12 Niskin  
120 bottles, for determining particulate organic carbon (POC), chlorophyll *a* (chl *a*) and  
121 phytoplankton biomass. Concentration values of POC, chl *a* and phytoplankton biomass  
122 in the water column, are integrated over the first 12 m depth, coinciding with the length

123 of the ropes where mussels grow. Integration was done at 1 m intervals from sea surface  
124 down to 12 m depth.

125 Vertical fluxes of particulate matter were measured by means of a sediment trap  
126 system MULTITRAP, with 4 cylindrical collectors with a height/diameter ratio of 10.8.  
127 At both stations, collectors were placed at a depth of 13 m, without adding any  
128 preservative and filled with a saline solution (5 psu in excess) to prevent water exchange  
129 with outside waters. Sediment traps remained deployed for 24 h at ReS and 3 h at RaS,  
130 to avoid silting the collectors due to expected high vertical fluxes under the raft. The  
131 sediment trap efficiency depends on the flow velocity. Baker et al. (1988) estimated that  
132 with currents less than  $12 \text{ cm s}^{-1}$ , the fluxes of matter collected by a sediment trap are  
133 equivalent to those collected by a drifting trap. In our study, current meters at the study  
134 sites recorded speeds below  $12 \text{ cm s}^{-1}$  for more than 90 % of the mooring time for the  
135 trap depths (Villacieros-Robineau, pers. comm.). Thus, we assume that potential biases  
136 in sedimentation fluxes are very low.

137 Samples for the analysis of POC, both in the water column (250 ml) and sediment  
138 traps (200 ml), were filtered through GF/F Whatman filters (0.7  $\mu\text{m}$  pore size),  
139 previously weighed and combusted at  $450 \text{ }^\circ\text{C}$  (4 h). Filters, after being dried overnight,  
140 were stored frozen until analysis. POC final concentrations were obtained using a  
141 PERKIN\_ELMER 2400 CNH elemental analyzer, including daily acetanilide standards.  
142 The accuracy of the method is  $\pm 0.3 \mu\text{mol C l}^{-1}$ .

143 Chl *a* concentration was determined by filtering samples of water column (250 ml)  
144 and sediment traps (200 ml) through GF/F Whatman filters. Immediately after filtration,  
145 filters were frozen ( $-20 \text{ }^\circ\text{C}$ ) until analysis. Prior to analysis, the filters were immersed in  
146 90 % acetone, leaving them for 24 h in darkness at  $4 \text{ }^\circ\text{C}$  for pigment extraction. The

147 final concentration of chl *a* was determined by measuring the fluorescence of the  
148 extracted pigments using a Turner Designs Fluorometer calibrated with pure chl *a*  
149 (Sigma Chemical).

150 From every depth of the water column and from two of the four sediment trap  
151 collectors, 100 ml samples were collected to estimate the carbon biomass of living  
152 phytoplankton cells in the water column and in the sediment traps. Samples were  
153 preserved in iodine solution and depending on chl *a* concentration, between 5 and 100  
154 ml of sample were settled using sedimentation chambers. An inverted microscope was  
155 used for counting and identification of phytoplankton cells, reaching the species level  
156 whenever possible. For simplicity, we apply the term phytoplankton to denote the set of  
157 autotrophic and heterotrophic microplankton (20 – 200  $\mu\text{m}$ ) identified by this means.  
158 Chain-forming diatoms (< 20  $\mu\text{m}$ ) were also ascribed to microplankton. The smaller  
159 species (< 20  $\mu\text{m}$ ) were counted doing one or two perpendicular transects with 400x  
160 magnification, medium individual (20 – 50  $\mu\text{m}$ ) were counted in one or two  
161 perpendicular transects using 200x magnification and larger organisms within  
162 phytoplankton (> 50  $\mu\text{m}$ ) were counted by scanning across the board with 100x  
163 magnification. At least 500 cells were counted in each sample. Cell biovolumes were  
164 calculated as recommended by Hillebrand (1999) and the biovolumes of diatoms and  
165 dinoflagellates were converted into carbon biomass according to Strathmann (1967).  
166 However, the estimation of cell carbon in *Noctiluca scintillans* was conducted by  
167 applying the correction suggested by Tada et al. (2000). Cellular carbon in flagellates,  
168 other than dinoflagellates, was estimated according Verity et al. (1992) and in ciliates  
169 according Putt and Stoecker (1989). Unfortunately, due to technical problems  
170 encountered during autumn sampling, we do not have the data set of chl *a* flux at ReS  
171 station, nor chl *a* and C<sub>phyto</sub> flux at RaS during this period.

## 172 2.2. Ekman transport and Runoff

173 We analyzed the intensity of upwelling based on the upwelling index, which was  
174 estimated using the component ( $-Q_x$ ,  $m^3 s^{-1} km^{-1}$ ) of the Ekman transport, that is  
175 perpendicular to the coast and hence equivalent to the surface water outflow from the  
176 Ría, following Bakun (1973):

$$177 \quad -Q_x = -[(\rho_a C |V|) / (f \rho_{sw})] V_y \quad (1)$$

178 where  $\rho_a$  is the air density ( $1.22 kg m^{-3}$ ) at  $15^\circ C$ ,  $C$  is an empirical coefficient of drag  
179 ( $1.3 \times 10^{-3}$ , dimensionless),  $|V|$  is the daily mean value of the module of the wind stress  
180 ( $m s^{-1}$ ) of northerly component ( $V_y$ ) registered by the Silleiro buoy deployed on the  
181 **shelf in front of the Ría de Vigo by ‘Puertos del Estado’**,  $f$  is the Coriolis parameter  
182 ( $9.95 \times 10^{-5} s^{-1}$ ) at  $43^\circ N$  and  $\rho_{sw}$  is the density of seawater ( $1025 kg m^{-3}$ ). Positive  
183 values of  $-Q_x$  indicate the predominance of northerly winds responsible for upwelling  
184 within the Ría, while negative values are related to downwelling induced by southerly  
185 winds.

186 Continental runoff into the inner part of the Ría de Vigo ( $Q_r$ ,  $m^3 s^{-1}$ ) is dominated by  
187 the discharge from the river Oitavén-Verdugo (Fig. 1). Daily flows were provided by  
188 **‘Aguas de Galicia’ (the company in charge of the management of urban waters)**. The  
189 natural component of the flow per unit area was calculated according to the empirical  
190 equation of Ríos et al. (1992).

## 191 2.3. Statistical analysis

192 To detect the significant differences between the observed sedimentation fluxes at  
193 ReS and at RaS, the non-parametric analysis of variance (Kruskal-Wallis test) was used.  
194 Statistical analysis was performed using the statistical software SPSS.



195 3. RESULTS

196 3.1. Biogeochemical properties of the water column at ReS

197 The observed variability in integrated POC, chl *a* and C<sub>phyto</sub> concentrations at ReS  
198 for the four study periods (Fig. 2, Table 1) was closely linked with the hydrographic  
199 changes previously analyzed in detail by Froján et al. (2014). The highest seasonal  
200 average POC concentration occurred in autumn ( $3531 \pm 803 \text{ mg m}^{-2}$ , Table 1), when  
201 transition from upwelling to downwelling conditions took place (Fig. 2a).  
202 Concentrations of C<sub>phyto</sub> and chl *a* followed a similar pattern to POC and the  
203 contribution of C<sub>phyto</sub> amounted on average about a half of POC ( $55 \pm 32 \%$ ). Diatoms  
204 were the largest biomass contributors to C<sub>phyto</sub> ( $66 \pm 22 \%$ ), with an outstanding  
205 presence of *Chaetoceros socialis* (Fig. 4).

206 During winter, the studied variables recorded annual minimum concentrations.  
207 Average POC in winter ( $1923 \pm 443 \text{ mg m}^{-2}$ ) was almost half of average POC obtained  
208 for the other three sampling periods (Table 1). Along with low chl *a* concentration ( $17 \pm$   
209  $5 \text{ mg m}^{-2}$ ), phytoplankton biomass also decreased, so its contribution to POC ( $11 \pm 4 \%$ )  
210 was considerably reduced. Diatoms continued to be the major component of  
211 phytoplankton community ( $53 \pm 8 \%$ ). The most prominent representative was the  
212 chain-forming species *Skeletonema cf. costatum* (Fig. 4).

213 During spring, C<sub>phyto</sub> ( $2294 \pm 1057 \text{ mg m}^{-2}$ ) and chl *a* ( $66 \pm 30 \text{ mg m}^{-2}$ )  
214 concentrations reaching the highest average values of all periods (Fig. 2b). Under these  
215 conditions, POC was largely made up of C<sub>phyto</sub> ( $67 \pm 20 \%$ ). Diatoms biomass  
216 dominated ( $67 \pm 14 \%$ ). *Detonula pumila* was the species that contributed the most in

217 the first half of the period, under low wind-high mixing conditions, while *Chaetoceros*  
218 *curvisetus* flourished after the strong river discharge (Fig. 4).

219 In summer, the three biogeochemical variables followed a similar evolution  
220 modulated by alternation of upwelling and relaxation events. Average concentrations  
221 and C<sub>phyto</sub>:POC ratio were lower than in autumn and spring. Dinoflagellates provided  
222 most of the biomass ( $62 \pm 13$  %) due to the contribution of the oversized dinoflagellate  
223 *Noctiluca scintillans* (Fig. 4).

### 224 3.2. Sedimentation flux at ReS

225 Flux of POC barely fluctuated during autumn ( $640 \pm 100$  mg m<sup>-2</sup> d<sup>-1</sup>; Table 2) despite  
226 changes in upwelling conditions (Fig. 3). Similarly, C<sub>phyto</sub> flux was high and steady,  
227 being the largest contribution to POC for the four studied periods ( $23 \pm 12$  %). Diatoms  
228 accounted for  $49 \pm 15$  % of biomass collected in the sediment traps. *Chaetoceros*  
229 *socialis*, *Chaetoceros curvisetus* and *Asterionellopsis glacialis* provided most of the  
230 biomass while the upwelling lasted. However, ciliates, dinoflagellates cysts and  
231 *Thalassiosira* sp. accounted for more than a half of the phytoplankton biomass after the  
232 strong downwelling (Fig. 3c, 4).

233 The POC flux during winter ( $633 \pm 183$  mg m<sup>-2</sup> d<sup>-1</sup>) hardly differed from the autumn  
234 one, but it reached minimum seasonal values for C<sub>phyto</sub> ( $55 \pm 15$  mg m<sup>-2</sup> d<sup>-1</sup>) and chl *a*  
235 ( $4 \pm 1$  mg m<sup>-2</sup> d<sup>-1</sup> ; Table 2). Therefore, C<sub>phyto</sub> content in POC flux ( $10 \pm 4$  %) was also  
236 low during this period. More than half of phytoplankton cells collected in the traps was  
237 diatoms ( $57 \pm 27$  %), mainly *Skeletonema* cf. *costatum* (Fig. 4).

238 Average POC flux in spring ( $924 \pm 445$  mg m<sup>-2</sup> d<sup>-1</sup>) was the annual highest (Fig. 3b).  
239 Chl *a* flux showed greater variability than C<sub>phyto</sub> flux, which was relatively low and

240 constant. Precisely, given the large POC flux of this period, Cphyto:POC ratio was  
241 similar to that found in winter ( $11 \pm 6$  %). Moreover, there was a high contribution of  
242 diatoms biomass ( $60 \pm 20$  %). *Detonula pumila* and *Leptocylindrus danicus* were the  
243 species that provided more biomass at the beginning, under mixing conditions, while  
244 the diatom *Chaetoceros curvisetus* thrived associated to large river input (Fig. 4).

245 Average summer POC flux was high ( $728 \pm 185$  mg m<sup>-2</sup> d<sup>-1</sup>), though not as much as  
246 the spring one (Fig. 3b). However, average Cphyto flux ( $115 \pm 84$  mg m<sup>-2</sup> d<sup>-1</sup>) was  
247 slightly higher than in the previous sampling, resulting in a Cphyto:POC ratio  
248 considerably higher ( $18 \pm 17$  %). Dinoflagellates became more important during this  
249 period, contributing  $38 \pm 22$  % of the biomass flux (Table 2), mostly due to *Noctiluca*  
250 *scintillans* (Fig. 4).

### 251 3.3. Biogeochemical properties of the water column at RaS

252 During autumn, suspended POC concentration at RaS ( $2526 \pm 666$  mg m<sup>-2</sup>) was on  
253 average  $27 \pm 17$  % lower than at ReS (Fig. 5, Table 1), being the only period with  
254 significant differences in POC concentration between the two sampling stations  
255 (Kruskal-Wallis test,  $p < 0.05$ ). Likewise, Cphyto ( $508 \pm 369$  mg m<sup>-2</sup>) and chl *a* ( $28 \pm$   
256  $19$  mg m<sup>-2</sup>) concentrations at RaS were significantly lower than at ReS. These changes  
257 resulted in a considerable reduction in the Cphyto:POC ratio at RaS ( $20 \pm 11$  %).  
258 Despite the general decline in Cphyto, diatoms continued to dominate ( $59 \pm 15$  %), with  
259 an important presence of *Chaetoceros socialis* (Fig. 4, 5c).

260 During winter, POC ( $1650 \pm 344$  mg m<sup>-2</sup>), Cphyto ( $130 \pm 41$  mg m<sup>-2</sup>) and chl *a* ( $11 \pm$   
261  $3$  mg m<sup>-2</sup>) concentrations in the water column at RaS reached the annual minima and  
262 were generally lower than at ReS. Furthermore, Cphyto:POC ratio at RaS ( $8 \pm 3$  %) was

263 even lower than at ReS (Table 1). Also, the proportion of diatom biomass at RaS  
264 decreased ( $48 \pm 10 \%$ ), though *Skeletonema cf. costatum* remained the most important  
265 species (Fig. 4).

266 The highest concentrations of POC ( $3111 \pm 427 \text{ mg m}^{-2}$ ), Cphyto ( $1575 \pm 941 \text{ mg}$   
267  $\text{m}^{-2}$ ) and chl *a* ( $54 \pm 19 \text{ mg m}^{-2}$ ) at RaS were reached in the spring sampling. Under  
268 these conditions, about half of POC was attributable to Cphyto ( $49 \pm 26 \%$ ), a  
269 contribution slightly lower than that observed at ReS, with diatoms accounting for  $> 70$   
270 % of the biomass. Similarly to ReS, *Detonula pumila* and *Chaetoceros curvisetus* were  
271 the most important species during this period (Fig. 4).

272 During summer, the Cphyto concentration at RaS ( $739 \pm 520 \text{ mg m}^{-2}$ ) was  
273 significantly lower (by  $48 \pm 21 \%$ ) than at ReS (Kruskal–Wallis test,  $p < 0.05$ ). Besides,  
274 Cphyto:POC ratio in the water column at RaS ( $35 \pm 26 \%$ ) was lower than at ReS. The  
275 proportion of dinoflagellates at RaS was high, and as observed at ReS, *Noctiluca*  
276 *scintillans* was the most important species during this period (Fig. 4).

#### 277 3.4. Sedimentation flux at RaS

278 Average POC flux at RaS during autumn ( $2507 \pm 2031 \text{ mg m}^{-2} \text{ d}^{-1}$ ) far exceeded the  
279 flux recorded at ReS (Table 2). Maximum POC flux values were recorded at the  
280 beginning of the period, and decreased to four times its value for the second half (Fig.  
281 6b). Unfortunately, we only have data of Cphyto and chl *a* fluxes at RaS for the first  
282 autumn sampling day.

283 In winter, average POC flux ( $1203 \pm 975 \text{ mg m}^{-2} \text{ d}^{-1}$ ) at RaS (Fig. 6b, Table 2) was  
284 the lowest of the year and showed no significant differences with ReS (Kruskal–Wallis  
285 test,  $p > 0.05$ ). Nor we did find significant differences in chl *a* flux, which was very

286 similar at the two stations. Nevertheless, Cphyto flux at RaS ( $22 \pm 14 \text{ mg m}^{-2} \text{ d}^{-1}$ ) was  
287 significantly lower than at ReS (Kruskal–Wallis test,  $p < 0.05$ ) and its contribution to  
288 POC ( $3 \pm 4 \%$ ) was also substantially lower. Although *Skeletonema* cf. *costatum* was  
289 the species with the highest biomass in the water column (Fig. 4), more than half of the  
290 biomass flux at RaS ( $54 \pm 23 \%$ ) was due to dinoflagellates and dinoflagellates cysts  
291 (Table 2, Fig. 4).

292 During spring, the highest seasonal average fluxes of POC ( $3958 \pm 1871 \text{ mg m}^{-2} \text{ d}^{-1}$ ),  
293 Cphyto ( $412 \pm 269 \text{ mg m}^{-2} \text{ d}^{-1}$ ) and chl *a* ( $125 \pm 101 \text{ mg m}^{-2} \text{ d}^{-1}$ ) were recorded, being  
294 significantly higher than at ReS (Kruskal–Wallis test,  $p < 0.05$ ). Cphyto contribution to  
295 POC flux ( $12 \pm 5 \%$ ) was relatively low during this period and similar to ReS. In terms  
296 of biomass, diatoms were the main contributors to Cphyto flux ( $77 \pm 15 \%$ ), with  
297 *Detonula pumila* and *Chaetoceros curvisetus* frequently appearing in the sediment traps  
298 at RaS (Fig. 4).

299 In summer, POC flux ( $2590 \pm 2026 \text{ mg m}^{-2} \text{ d}^{-1}$ ) was highly variable at RaS and  
300 significantly higher than at ReS (Kruskal–Wallis test,  $p < 0.05$ ). However, Cphyto flux  
301 at RaS ( $182 \pm 135 \text{ mg m}^{-2} \text{ d}^{-1}$ ) was not significantly different from ReS. Consequently,  
302 Cphyto:POC ratio at RaS was lower ( $10 \pm 12 \%$ ). As at ReS, diatoms provided an  
303 important part of the biomass collected in sediment traps ( $39 \pm 26 \%$ ), especially the  
304 species *Chaetoceros curvisetus*, *Lauderia annulata*, *Leptocylindrus danicus* and  
305 *Coscinodiscus* sp. Dinoflagellates maintained a high biomass flux at RaS ( $49 \pm 23 \%$ ),  
306 higher than at ReS ( $38 \pm 22 \%$ ), whose foremost representative remained *Noctiluca*  
307 *scintillans* (Fig. 4).

308

## 309 4. DISCUSSION

### 310 4.1. Vertical export of phytoplankton carbon

311 Considering that the structure and composition of the microbial community in the  
312 ocean involves a certain degree of autotrophy of the system and therefore a certain  
313 export capacity (Smith and Kemp 2001; Cermeño et al. 2006; Arbones et al. 2008), in  
314 this study we focused on unravelling to what extent changes in quantity and quality of  
315 phytoplankton biomass in the water column can modulate the vertical export of organic  
316 carbon outside the photic layer, and how this export is modified by the presence of  
317 mussel farming.

318 The present study showed that the seasonal variability of suspended POC (Fig. 7a,  
319 Table 1) was not reflected in the magnitude of POC vertical flux, since it remained  
320 relatively constant with an annual average of  $731 \pm 276 \text{ mg m}^{-2} \text{ d}^{-1}$ , and with no  
321 significant differences between periods (Fig. 7b, Table 2). However, we did find  
322 variability in the composition of POC collected in the traps, due to variability in C<sub>phyto</sub>  
323 flux (Fig. 7b, c). In this way, between 9 and 31 % of POC flux at ReS was due to  
324 C<sub>phyto</sub> flux, similar to previously published results for the Ría de Pontevedra and Vigo  
325 (2 – 26%), (Varela et al. 2004; Zúñiga et al. 2011). Likewise, diatom contribution to  
326 vertical C<sub>phyto</sub> flux varied over the different periods (35 – 69 %). This seasonal  
327 variation in quantity and quality of C<sub>phyto</sub> points to a vertical flux modulated by the  
328 different composition of phytoplankton community in the water column and the  
329 changing oceanographic scenarios (Fig. 8).

330 In fact, during our study year the two contrasting situations regarding export capacity  
331 of phytoplankton living cells corresponded to the autumn and winter cruises. The largest

332 Cphyto fluxes at ReS were achieved during the upwelling to downwelling autumn  
333 transition, associated with the presence of large and chain-forming diatoms, responsible  
334 for the high export capacity of the system. In this way, initial upwelling conditions  
335 favored diatoms bloom followed by subsequent sinking of chain-forming species  
336 (*Chaetoceros socialis*, *Chaetoceros curvisetus* and *Asterionellopsis glacialis*; Fig. 8).  
337 By contrast, during the winter mixing, annual minimum levels of Cphyto in the water  
338 column resulted in the lowest Cphyto fluxes of the year. Nevertheless, the proportion of  
339 diatoms in the traps ( $57 \pm 27$  %) reflected Cphyto composition in the water column (Fig.  
340 7a, b), where long chains of the diatom *Skeletonema* cf. *costatum* were vertically  
341 exported (Fig. 8).

342 In between these two contrasting cases of Cphyto flux, minimum for winter and  
343 maximum for autumn, the intermediate export capacities for the spring and summer  
344 cruises also responded to prevailing hydrographic conditions (higher or lower degree of  
345 stratification) and the composition of the microbial community. Under the well mixed  
346 water column of the spring sampling, long chains of diatoms predominated (*Detonula*  
347 *pumila* and *Leptocylindrus danicus*) (Fig. 8a). These large and chain-forming species  
348 present a high export capacity, being identified in the sinking material together with  
349 dinoflagellates cysts, which indicated the occurrence of surface sediment resuspension  
350 (Fig. 8b). The subsequent thermohaline stratification resulted in the proliferation of the  
351 chain-forming diatom *Chaetoceros curvisetus* (Fig. 8a) with relatively low contribution  
352 to the settling material ( $9 \pm 6$  %, Fig. 7b). This low share could be related with the  
353 morphologically favored buoyancy of *Ch. curvisetus* (Margalef 1978; Tilstone et al.  
354 2000; Acuña et al. 2010), but also with intense water column stratification that hinders  
355 vertical flux, and favors the potential horizontal offshore advection as a result of the  
356 positive circulation reinforced by river discharge (Varela et al. 1991; Castro et al. 1994).

357 On the other hand, the buoyancy or swimming ability of *Noctiluca scintillans* (Fermín  
358 et al. 1996) likely favored the accumulation of this oversized heterotrophic  
359 dinoflagellate during the summer sampling (Fig. 8a). However, the contribution of  
360 Cphyto to POC in sediment traps ( $18 \pm 17$  %, Fig. 7b), was relatively low compared  
361 with water column ( $54 \pm 33$  %, Fig. 7a), indicating that an important part of the fixed  
362 carbon was not vertically exported, being probably consumed by *Noctiluca scintillans*  
363 (Kiørboe et al. 1998; Tiselius and Kiørboe 1998).

364 Thus, the composition of phytoplankton community, together with hydrodynamic  
365 processes modulates the vertical export of biogenic particles in the Ría de Vigo. The  
366 largest Cphyto fluxes at ReS were achieved during the autumn transition from  
367 upwelling to downwelling conditions, associated with high NCP ( $186 \pm 67$  mmol O<sub>2</sub> m<sup>-2</sup>  
368 d<sup>-1</sup>; Froján et al. submitted), and the presence of large and chain-forming diatoms,  
369 responsible for the high export capacity of the system. By contrast, during the winter  
370 mixing we found lower Cphyto fluxes associated with a lesser degree of autotrophy ( $43$   
371  $\pm 22$  mmol O<sub>2</sub> m<sup>-2</sup> d<sup>-1</sup>).

#### 372 4.2. Influence of mussel farming in vertical export of phytoplankton carbon

373 Studies conducted in the Galician Rías have showed high sedimentation rates in the  
374 rafts area (Cabanas et al. 1979; Tenore et al. 1982; Alonso-Pérez et al. 2010; Zúñiga et  
375 al. 2014) due to mussel biodeposits flux. Our results corroborates these previous works,  
376 since we have observed an average POC flux at RaS ( $2564 \pm 1936$  mg m<sup>-2</sup> d<sup>-1</sup>) four  
377 times higher than at ReS ( $731 \pm 276$  mg m<sup>-2</sup> d<sup>-1</sup>). At the same time and in contrast to the  
378 pattern observed at ReS, the magnitude of the POC flux at RaS varied seasonally (Fig  
379 7e, Table 2). In this context, our study is the first to analyze in detail the seasonality in  
380 POC sedimentation under a mussel raft.



381 If we consider that much of the POC flux collected by sediment traps in the raft area  
382 was due to the contribution of biodeposits, the variability in the biodeposits flux could  
383 explain the observed variability in the POC flux at RaS. In this regard, little is known  
384 about the relative contribution of mussel biodeposits to vertical sedimentation fluxes,  
385 despite being essential to understand the influence of mussel farming in the ecosystem.  
386 Giles et al. (2006) indicated that between 6 and 14 % of the sediment flux in the  
387 farming area of a bay in New Zealand was due to mussel feces. In our study, to estimate  
388 the proportion of POC flux due to biodeposits at RaS, we distinguish three components  
389 of the POC flux collected by the sediment traps: biodeposits flux ( $C_{\text{biodep}}$ ),  $C_{\text{phyto}}$   
390 flux measured in the sedimentation traps at RaS ( $C_{\text{phyto}}$ ), and remaining particulate  
391 organic carbon flux ( $C_{\text{rest}}$ ), which we assume the same at the two sampling stations.

$$392 \quad \text{Flux}C_{\text{biodep}}^{\text{RaS}} = \text{FluxPOC}^{\text{RaS}} - \text{Flux}C_{\text{phyto}}^{\text{RaS}} - \text{Flux}C_{\text{rest}}^{\text{ReS}} \quad (2)$$

393 In this way, the observed differences in POC flux between ReS and RaS would be  
394 due to differences in  $C_{\text{phyto}}$  and  $C_{\text{biodep}}$  fluxes. Based on these calculations,  $C_{\text{biodep}}$   
395 flux accounted for  $58 \pm 32$  % of the POC flux in spring, and for  $60 \pm 19$  % in summer,  
396 being related with the significant increase of the POC flux observed in RaS regarding  
397 ReS in these periods (Kruskal-Wallis test,  $p < 0.05$ ). On the contrary, during winter,  
398 with a lower estimated  $C_{\text{biodep}}$  flux ( $35 \pm 39$  %), we did not find significant differences  
399 in the POC flux between the two sampling stations (Kruskal-Wallis test,  $p > 0.05$ ).  
400 Overall, our values are higher than those provide by Giles et al. (2006), but in line with  
401 a greater mussel production in our study region.

402 Indeed because of the high  $C_{\text{biodep}}$  flux in the raft area, only a small proportion of  
403 the POC flux was due to  $C_{\text{phyto}}$  flux (3 – 17%), (Fig. 7e, Table 2). If we also consider  
404 the decline in NCP at RaS observed by Froján et al. (submitted), we may expect a lower

405 Cphyto flux since it involves a smaller export capacity of the system. During winter, our  
406 assumption was met, with a significant reduction in the vertical exportation of Cphyto at  
407 RaS (Kruskal–Wallis test,  $p < 0.05$ ), that would be related to the reduction in Cphyto  
408 biomass in the water column as consequence of mussel feeding (Fig. 7). By contrast,  
409 Cphyto flux at Ras was higher than at ReS during spring and summer (Fig. 7c, f),  
410 though the differences were only significant in spring (Kruskal–Wallis test,  $p < 0.05$ ).  
411 In this context, we have identified a variety of mechanisms which would explain the  
412 increase in sedimentation of Cphyto at RaS.

413 First of all, our observations lead us to think that Cphyto flux at RaS in spring and  
414 summer could have been favored by the less energetic hydrodynamic conditions in the  
415 raft area, due to the decrease in the current velocity when passing through culture ropes  
416 (Blanco et al. 1996; Newell and Richardson 2014). Moreover, based on the fact that a  
417 high Cbiodep flux occurred at RaS both in spring and summer samplings, and that the  
418 average size of mussel feces exceeds 200  $\mu\text{m}$  (Giles and Pilditch 2004) we suggest that  
419 the settling of mussel feces could cause a ballast effect on other biogenic particles in the  
420 water column (Boyd and Trull 2007; Passow and Carlson 2012), increasing Cphyto  
421 fluxes. In principle, it can be expected that these mechanisms affect more those species  
422 with greater tendency to settle, as occurred in summer for large (*Coscinodiscus* sp.) and  
423 chain-forming diatoms (*Lauderia annulata*), that sedimented more at RaS (Fig. 4, 8d).  
424 But even species, whose morphological characteristics give them some buoyancy as  
425 *Noctiluca scintillans* in summer and *Chaetoceros curvisetus* in spring and summer,  
426 recorded increased sedimentation at RaS (Fig 4). In the particular case of *Ch.*  
427 *Curvisetus*, we think that the quietest hydrodynamic conditions in the raft area could  
428 even favor the formation of aggregates (Kranck and Milligan 1988; Alldredge and  
429 Gotschalk 1989), resulting from increase the adherence between cells by producing

430 exopolymers (Lancelot 1983; Kiørboe and Hansen 1993), and this could be a secondary  
431 factor contributing to explain the increase of sedimentation of this species at RaS (Fig.  
432 8d).

433 We also note that mussel farming not only altered the quantity of Cphyto flux, but  
434 also the quality, understood as the contribution of diatoms to Cphyto flux. At RaS, the  
435 proportion of diatoms in the traps was very similar to that found in the water column,  
436 and both proportions were significantly correlated ( $r^2 = 0.73$ ,  $p < 0.001$ ). By contrast at  
437 ReS, a greater variability can be seen, and it is striking the loss of the relationship  
438 between proportions observed at ReS ( $r^2 = 0.14$ ,  $p < 0.05$ ). One possible explanation for  
439 this lower variability at RaS, could be the reduction of zooplankton in the water column  
440 after being consumed by mussels (Maar et al. 2008). By removing the predatory  
441 pressure of zooplankton, feeding disturbance that zooplankters exerted on the  
442 distribution and composition of diatoms in the water column would be reduced,  
443 resulting in less variability in the composition of the vertical fluxes of diatoms collected  
444 in the sediment traps with regard to those found in the water column.

445 In short, this is the first study that analyzes the Cphyto flux under a mussel raft and  
446 proposes a combination of mechanisms that explain the increased sedimentation of  
447 phytoplankton cells in this area. As a result of this increase at RaS, the relationship  
448 between NCP and Cphyto that existed at ReS was lost. Thus, despite the decline in NCP  
449 because of top-down control by mussels on phytoplankton and the light attenuation  
450 under rafts (Froján et al. submitted), we observed that the export capacity increased in  
451 the raft area. Hence, our results indicate that mussel farming has a strong impact on  
452 sedimentation flux under the rafts, not only increasing the POC flux, but also altering  
453 the magnitude and composition of Cphyto fluxes. Additional research increasing

454 temporal and spatial resolution of sampling, both inside and outside the farming areas,  
455 is needed to further support our conclusions.

456

457

458

459

460

461

462

463

464

465

466

467

468

469

470

471 *Acknowledgements: We thank the crew of the ‘R/V Mytilus’ and the members of the*  
472 *oceanography group from the Instituto de Investigaci3n Mariñas de Vigo (CSIC) for*  
473 *their valuable help. Financial support came from MICINN RAFTING project*  
474 *(CTM2007-61983/MAR, CTM2007-30624-E/MAR). D. Z. was funded by a*  
475 *postdoctoral fellowship (Plan I2C) from Xunta de Galicia.*

476

477

478

479

480

481

482

483

484

485

486

487

488

489

490

491

492

493

494

495

496 REFERENCES

- 497 Acuña, J.L., M. López-Álvarez, E. Nogueira, and F. González-Taboada. 2010. Diatom  
498 flotation at the onset of the spring phytoplankton bloom: an in situ experiment.  
499 *Marine Ecology Progress Series* 400: 115–125.
- 500 Alldredge, A.L., and C. Gotschalk. 1989. Direct observations of the mass flocculation  
501 of diatoms blooms: Characteristics, settling velocities and formation of marine  
502 snow. *Deep Sea Research* 36: 159–171.
- 503 Alonso-Pérez, F., T. Ysebaert, and C.G. Castro. 2010. Effects of suspended mussel  
504 culture on benthic–pelagic coupling in a coastal upwelling system (Ría de Vigo,  
505 NW Iberian Peninsula). *Journal of Experimental Marine Biology and Ecology* 382:  
506 96–107.
- 507 Arbones, B., C.G. Castro, F. Alonso-Pérez, and F.G. Figueiras. 2008. Phytoplankton  
508 size structure and water column metabolic balance in a coastal upwelling system:  
509 the Ría de Vigo, NW Iberia. *Aquatic Microbial Ecology* 50: 169–179.
- 510 Baker, E.T., H.B. Milburn, and D.A. Tennant. 1988. Field assessment of sediment trap  
511 efficiency under varying flow conditions. *Journal of Marine Research* 46: 573–  
512 592.
- 513 Bakun, A. 1973. Coastal upwelling indices, west coast of North America, 1946–71.  
514 *NOAA Technical Report NMFS SSRF-671*.
- 515 Blanco, J., M. Zapata, and A. Moróño. 1996. Some aspects of the water flow through  
516 mussel rafts. *Scientia Marina* 60: 275–282.
- 517 Blanton, J. O., K.R. Tenore, F. Castillejo, L.P. Atkinson, F.B. Schwing and A. Lavin.  
518 1987. The relationship of upwelling to mussel production in the rias on the western  
519 coast of Spain. *Journal of Marine Research* 45:497–511.
- 520 Bode, A., M. Varela, S. Barquero, M.T. Ossorio-Alvarez, and N. González. 1998.  
521 Preliminary Studies on the Export of Organic Matter During Phytoplankton  
522 Blooms off La Coruña (Northwestern Spain). *Journal of the Marine Biological*  
523 *Association of the United Kingdom* 78. Cambridge University Press: 1–15.
- 524 Boyd, P.W., and T.W. Trull . 2007. Understanding the export of biogenic particles in  
525 oceanic waters: is there consensus? *Progress in Oceanography* 72: 276–312.
- 526 Buesseler, K.O. 1998. The decoupling of production and particulate export in the  
527 surface ocean. *Global Biogeochemical Cycles* 12: 297–310.
- 528 Cabanas, J.M., J.J. González, J.J. Mariño, A Pérez Camacho, and G Boland. 1979.  
529 Estudio del mejillón y de su epifauna asociada en los cultivos flotantes de la Ría de  
530 Arosa. III. Observaciones preliminares sobre la retención de partículas y la  
531 biodeposición de un batea. *Boletín Instituto Español Oceanografía* 5: 45–50.

- 532 Callier, M.D., A.M. Weise, C.W. McKindsey, and G. Desrosiers. 2006. Sedimentation  
533 rates in a suspended mussel farm (Great-Entry Lagoon, Canada): Biodeposit  
534 production and dispersion. *Marine Ecology Progress Series* 322: 129–141.
- 535 Castro, C.G., F.F. Pérez, X.A. Álvarez-Salgado, G. Rosón, and A.F. Ríos. 1994.  
536 Hydrographic conditions associated with the relaxation of an upwelling event off  
537 the Galician coast (NW Spain). *Journal of Geophysical Research* 99: 5135–5147.
- 538 Cermeño, P., E. Marañón, V. Pérez, P. Serret, E. Fernández, and C.G. Castro. 2006.  
539 Phytoplankton size structure and primary production in a highly dynamic coastal  
540 ecosystem (Ría de Vigo, NW-Spain): Seasonal and short-time scale variability.  
541 *Estuarine, Coastal and Shelf Science* 67: 251–256.
- 542 Cranford, P.J., M. Dowd, and J. Grant. 2003. Ecosystem level effects of marine bivalve  
543 aquaculture. *Canadian Technical Reports of Fisheries and Aquatic Sciences* 2450:  
544 51–96.
- 545 Cranford, P.J., B.T. Hargrave, and L.I. Doucette. 2009. Benthic organic enrichment  
546 from suspended mussel (*Mytilus edulis*) culture in Prince Edward Island, Canada.  
547 *Aquaculture* 292: 189–196.
- 548 Crespo, B.G., F.G. Figueiras, P. Porras, and I.G. Teixeira. 2006. Downwelling and  
549 dominance of autochthonous dinoflagellates in the NW Iberian margin: The  
550 example of the Ría de Vigo. *Harmful Algae* 5:770–781.
- 551 Dahlbäck, B., and L.Å.H. Gunnarsson. 1981. Sedimentation and sulfate reduction under  
552 a mussel culture. *Marine Biology* 63: 269–275.
- 553 Dame, R.F. 1996. *Ecology of marine bivalves: an ecosystem approach*. Boca Raton, FL:  
554 CRC Press.
- 555 Fermín, E.G., F.G. Figueiras, B. Arbones, and M.L. Villarino. 1996. Short-time scale  
556 development of a *Gymnodinium catenatum* population in the Ría de Vigo (NW  
557 Spain). *Journal of phycology* 32: 212–221.
- 558 Figueiras, F.G., U. Labarta, and M.J. Fernández-Reiriz. 2002. Coastal upwelling,  
559 primary production and mussel growth in the Rías Baixas of Galicia.  
560 *Hydrobiologia* 484: 121–131.
- 561 Fowler, S.W., and G.A. Knauer. 1986. Role of large particles in the transport of  
562 elements and organic compounds through the oceanic water column. *Progress in*  
563 *Oceanography* 16: 147–194.
- 564 Froján, M., B. Arbones, D. Zúñiga, C.G. Castro, and F.G. Figueiras. 2014. Microbial  
565 plankton community in the Ría de Vigo (NW Iberian upwelling system): impact of  
566 the culture of *Mytilus galloprovincialis*. *Marine Ecology Progress Series* 498: 43–  
567 54.
- 568

- 569 Froján, M., C.G. Castro, D. Zúñiga, B. Arbones, F. Alonso-Pérez, and F.G. Figueiras.  
570 (Submitted). Mussel farming impact on the pelagic production and respiration rates  
571 in the Ría de Vigo (NW Iberian upwelling).
- 572 Giles, H., and C.A. Pilditch. 2004. Effects of diet on sinking rates and erosion  
573 thresholds of mussel *Perna canaliculus* biodeposits. *Marine Ecology Progress*  
574 *Series* 282: 205–219.
- 575 Giles, H., C.A. Pilditch, and D.G. Bell. 2006. Sedimentation from mussel (*Perna*  
576 *canaliculus*) culture in the Firth of Thames, New Zealand: Impacts on sediment  
577 oxygen and nutrient fluxes. *Aquaculture* 261: 125–140.
- 578 Hillebrand, H., C.-D. Dürselen, D. Kirschtel, U. Pollinger, and T. Zohary. 1999.  
579 Biovolume calculation for pelagic and benthic microalgae. *Journal of Phycology*  
580 35: 403–424.
- 581 Jaramillo, E., C. Bertran, and A. Bravo. 1992. Mussel biodeposition in an estuary in  
582 southern Chile. *Marine Ecology Progress Series* 82: 85–94.
- 583 Kiørboe, T., and J.L.S. Hansen. 1993. Phytoplankton aggregate formation: Observations  
584 of patterns and mechanisms of cell sticking and the significance of exopolymeric  
585 material. *Journal of Plankton Research* 15: 993–1018.
- 586 Kiørboe, T., P. Tiselius, B. Mitchell-Hynes, J.L.S. Hansen, A.W. Visser, and X. Mari.  
587 1998. Intensive aggregate formation with low vertical flux during an upwelling–  
588 induced diatom bloom. *Limnology and Oceanography* 43: 104–116.
- 589 Kranck, K., and T.G. Milligan. 1988. Macroflocs from diatoms: in situ photography of  
590 particles in Bedford Basin, Nova Scotia. *Marine Ecology Progress Series* 44:  
591 183–189.
- 592 Lancelot, C. 1983. Factors affecting phytoplankton extracellular release in the Southern  
593 Bight of the North Sea. *Marine Ecology Progress Series* 12: 115–121.
- 594 Maar, M., T.G. Nielsen, and J.K. Petersen. 2008. Depletion of plankton in a raft culture  
595 of *Mytilus galloprovincialis* in Ría de Vigo, NW Spain. II. Zooplankton. *Aquatic*  
596 *Biology* 4: 127–141.
- 597 Margalef, R. 1978. Life-forms of phytoplankton as survival alternatives in an unstable  
598 environment. *Oceanologica Acta* 1: 493–509.
- 599 Newell, C.R., and J. Richardson. 2014. The Effects of Ambient and Aquaculture  
600 Structure Hydrodynamics on the Food Supply and Demand of Mussel Rafts.  
601 *Journal of Shellfish Research* 33: 257–272.
- 602 Nogueira, E., and F.G. Figueiras. 2005. The microplankton succession in the Ría de  
603 Vigo revisited: species assemblages and the role of the weather-induced,  
604 hydrodynamic variability. *Journal of Marine Systems* 54:139–155.



- 605 Nogueira, E., F. Ibanez, and F.G. Figueiras. 2000. Effect of meteorological and  
606 hydrographic disturbances on the microplankton community structure in the Ría de  
607 Vigo (NW Spain). *Marine Ecology Progress Series* 203:23–45.
- 608 Olli, K., C. Wexels Riser, P. Wassmann, T. Ratkova, E. Arashkevich, and A. Pasternak.  
609 2001. Vertical flux of biogenic matter during a Lagrangian study off the NW  
610 Spanish continental margin. *Progress in Oceanography* 51: 443–466.
- 611 Passow, U. and C.A. Carlson. 2012. The biological pump in a high CO<sub>2</sub> World. *Marine  
612 Ecology Progress Series* 470: 249–271.
- 613 Pérez-Camacho, A., U. Labarta, V. Vinseiro, M.J. Fernández-Reiriz. 2013. Mussel  
614 production management: Raft culture without thinning-out. *Aquaculture* 406–  
615 407:172–179.
- 616 Putt, M., and D.K. Stoecker. 1989. An experimentally determined carbon : **volume ratio**  
617 **for marine “oligotrichous” ciliates from estuarine and coastal waters.** *Limnology  
618 and Oceanography* 34: 1097–1103.
- 619 Ríos, A.F., M.A. Nombela, F.F. Pérez, G. Rosón, and F. Fraga. 1992. Calculation of  
620 runoff to an estuary. Ria de Vigo. *Scientia Marina* 56: 29–33.
- 621 Smith, E.M., and W.M. Kemp. 1995. Seasonal and regional variations in plankton  
622 community production and respiration for Chesapeake Bay. *Marine Ecology  
623 Progress Series* 116: 217–232.
- 624 Smith, E.M., and W.M. Kemp. 2001. Size structure and the production/respiration  
625 balance in a coastal plankton community. *Limnology and Oceanography* 46: 473–  
626 485.
- 627 Strathmann, R.R. 1967. Estimating the organic carbon content of phytoplankton from  
628 cell volume or plasma volume. *Limnology and Oceanography* 12: 411–418.
- 629 Tada, K., S. Pithakpol, R. Yano, and S. Montani. 2000. Carbon and nitrogen content of  
630 *Noctiluca scintillans* in the Seto Inland Sea, Japan. *Journal of Plankton Research*  
631 22: 1203–1211.
- 632 Tenore, K.R., L.F. Boyer, R.M. Cal, J. Corral, C. Garcia-Fernandez, N. Gonzalez, E.  
633 Gonzalez-Gurriaran, R.B. Hanson, J. Iglesias, and J. Krom. 1982. Coastal  
634 Upwelling in the Rias Bajas Northwestern Spain Contrasting the Benthic Regimes  
635 of the Rias De Arosa and De Muros. *Journal of Marine Research* 40: 701–772.
- 636 Tilstone, G.H., B.M. Miguez, F.G. Figueiras, and E.G. Fermin. 2000. Diatom dynamics  
637 in a coastal ecosystem affected by upwelling: Coupling between species  
638 succession, circulation and biogeochemical processes. *Marine Ecology Progress  
639 Series* 205: 23–41.
- 640 Tiselius, P., and T. Kiørboe. 1998. Colonization of diatom aggregates by the  
641 dinoflagellate *Noctiluca scintillans*. *Limnology and Oceanography* 43: 154–159.

- 642 Tremblay, J.-É., and L. Legendre. 1994. A model for the size-fractionated biomass and  
643 production marine phytoplankton. *Limnology and Oceanography* 39: 2004–2014.
- 644 Turner, J.T. 2015. Zooplankton fecal pellets, marine snow, phytodetritus and the  
645 **ocean’s biological pump**. *Progress in Oceanography* 130: 205–248.
- 646 Varela, M., G. Díaz del Río, M.T. Álvarez-Ossorio, and E. Costas. 1991. Factors  
647 controlling phytoplankton size class distribution in the upwelling area of the  
648 Galician continental shelf (NW Spain). *Scientia Marina* 55: 505–518.
- 649 Varela, M., R. Prego, and Y. Pazos. 2004. Vertical biogenic particle flux in a western  
650 Galician ria (NW Iberian Peninsula). *Marine Ecology Progress Series* 269: 17–32.
- 651 Verity, P.G., C.Y. Robertson, C.R. Tronzo, M.G. Andrews, J.R. Nelson, and M.E.  
652 Sieracki. 1992. Relationships between cell volume and the carbon and nitrogen  
653 content of marine photosynthetic nanoplankton. *Limnology and Oceanography* 37:  
654 1434–1446.
- 655 Villaceros-Robineau, N., J.L. Herrera, C.G. Castro, S. Piedracoba, and G. Rosón. 2013.  
656 Hydrodynamic characterization of the bottom boundary layer in a coastal  
657 upwelling system (Ría de Vigo, NW Spain). *Continental Shelf Research* 68.  
658 Elsevier: 67–79.
- 659 Zúñiga, D., F. Alonso-Pérez, C.G. Castro, B. Arbones, and F.G. Figueiras. 2011.  
660 Seasonal contribution of living phytoplankton carbon to vertical fluxes in a coastal  
661 upwelling system (Ría de Vigo, NW Spain). *Continental Shelf Research* 31: 414–  
662 424.
- 663 Zúñiga, D., C.G. Castro, E. Aguiar, U. Labarta, F.G. Figueiras, and M.J. Fernández-  
664 Reiriz. 2014. Biodeposit contribution to natural sedimentation in a suspended  
665 *Mytilus galloprovincialis* Lmk mussel farm in a Galician Ría (NW Iberian  
666 Peninsula). *Aquaculture* 432: 311–320.

667  
668

669

670

671

672

673

674

675

676

677

678 FIGURE CAPTIONS

679

680 Fig. 1 Location map of the Ría de Vigo showing the two sampling sites (✱):  
681 Reference (ReS) and raft (RaS) stations. Raft polygons are shown as blue areas. Above,  
682 zoom in nearby the experimental raft showing the seawater sampling site (SW) and the  
683 location used for sediment trap deployments (ST) at RaS.

684

685 Fig. 2 (a) Time series of upwelling index (UI,  $\text{m}^3 \text{s}^{-1} \text{km}^{-1}$ , black bars) and river  
686 outflow ( $Q_r$ ,  $\text{m}^3 \text{s}^{-1}$ , grey bars), (b) particulate organic carbon (POC), phytoplankton  
687 carbon (C<sub>phyto</sub>), and chlorophyll *a* (chl *a*) integrated concentrations for the first 12 m  
688 of the water column at the reference station (ReS), (c) Bar plots of biomass of the main  
689 phytoplankton groups in the water column. Units ( $\text{mg m}^{-2}$ ).

690

691 Fig. 3 (a) Time series of upwelling index (UI,  $\text{m}^3 \text{s}^{-1} \text{km}^{-1}$ , black bars) and river  
692 outflow ( $Q_r$ ,  $\text{m}^3 \text{s}^{-1}$  grey bars), (b) particulate organic carbon (POC), phytoplankton  
693 carbon (C<sub>phyto</sub>), and chlorophyll *a* (chl *a*) vertical fluxes at the reference station (ReS),  
694 (c) Bar plots of biomass of the main phytoplankton group collected in the sediment  
695 traps. Units ( $\text{mg m}^{-2} \text{d}^{-1}$ ).

696

697 Fig. 4 Average integrated biomass of the main phytoplankton species in the water  
698 column (up bars,  $\text{mg C m}^{-2}$ ), and in the sediment traps (down bars,  $\text{mg C m}^{-2} \text{d}^{-1}$ ), at  
699 reference (ReS, black bars) and raft (RaS, gray bars) stations, for each sampling period  
700 (autumn, winter, spring and summer)

701

702 Fig. 5 (a) Time series of upwelling index (UI,  $\text{m}^3 \text{s}^{-1} \text{km}^{-1}$ , black bars) and river  
703 outflow ( $Q_r$ ,  $\text{m}^3 \text{s}^{-1}$ , grey bars), (b) particulate organic carbon (POC), phytoplankton  
704 carbon (C<sub>phyto</sub>), and chlorophyll *a* (chl *a*) integrated for the first 12 m of the water  
705 column at raft station (RaS), (c) Bar plots of the biomass of the main phytoplankton  
706 groups in the water column. Units ( $\text{mg m}^{-2}$ ).

707

708 Fig. 6 (a) Time series of upwelling index (UI,  $\text{m}^3 \text{s}^{-1} \text{km}^{-1}$ , black bars) and river  
709 outflow ( $Q_r$ ,  $\text{m}^3 \text{s}^{-1}$ , grey bars), (b) particulate organic carbon (POC), phytoplankton  
710 carbon (C<sub>phyto</sub>), and chlorophyll *a* (chl *a*) fluxes at raft station (RaS), (c) Bar plots of  
711 the biomass of the main phytoplankton group collected in the sediment traps. Units ( $\text{mg}$   
712  $\text{m}^{-2} \text{d}^{-1}$ )

713

714 Fig. 7 Stacked bars plot showing the relative contribution of diatoms (striped blue,  
715 % blue number) to C<sub>phyto</sub> (solid blue), and the relative contribution of C<sub>phyto</sub> (%  
716 white number) to POC (solid gray), both in the water column ( $\text{mg C m}^{-2}$ ) at reference (a,  
717 ReS) and raft (d, RaS) stations, and in the sediment traps ( $\text{mg C m}^{-2} \text{d}^{-1}$ ) at reference (b,  
718 ReS) and raft (e, RaS) stations. Below (c, ReS) and (f, RaS) zoom on the relative  
719 contribution of diatoms flux to C<sub>phyto</sub> flux. The stacked bars correspond to the  
720 different oceanographic scenarios: the first half of autumn (aut-1), the second half of  
721 autumn (aut-2), winter (win), the first half of spring (spr-1), the second half of spring  
722 (spr-2), and summer (sum)

723

724 Fig. 8 Schematic evolution of the phytoplankton annual cycle with the major  
725 phytoplankton species in biomass for each sampling period, both in the water column

726 (a, ReS), (b, RaS) and in the sediment traps (c, ReS), (d, RaS). Redrawn according to  
727 the seasonal scheme provided by Figueiras et al. (2002)

728

729

Figure 1

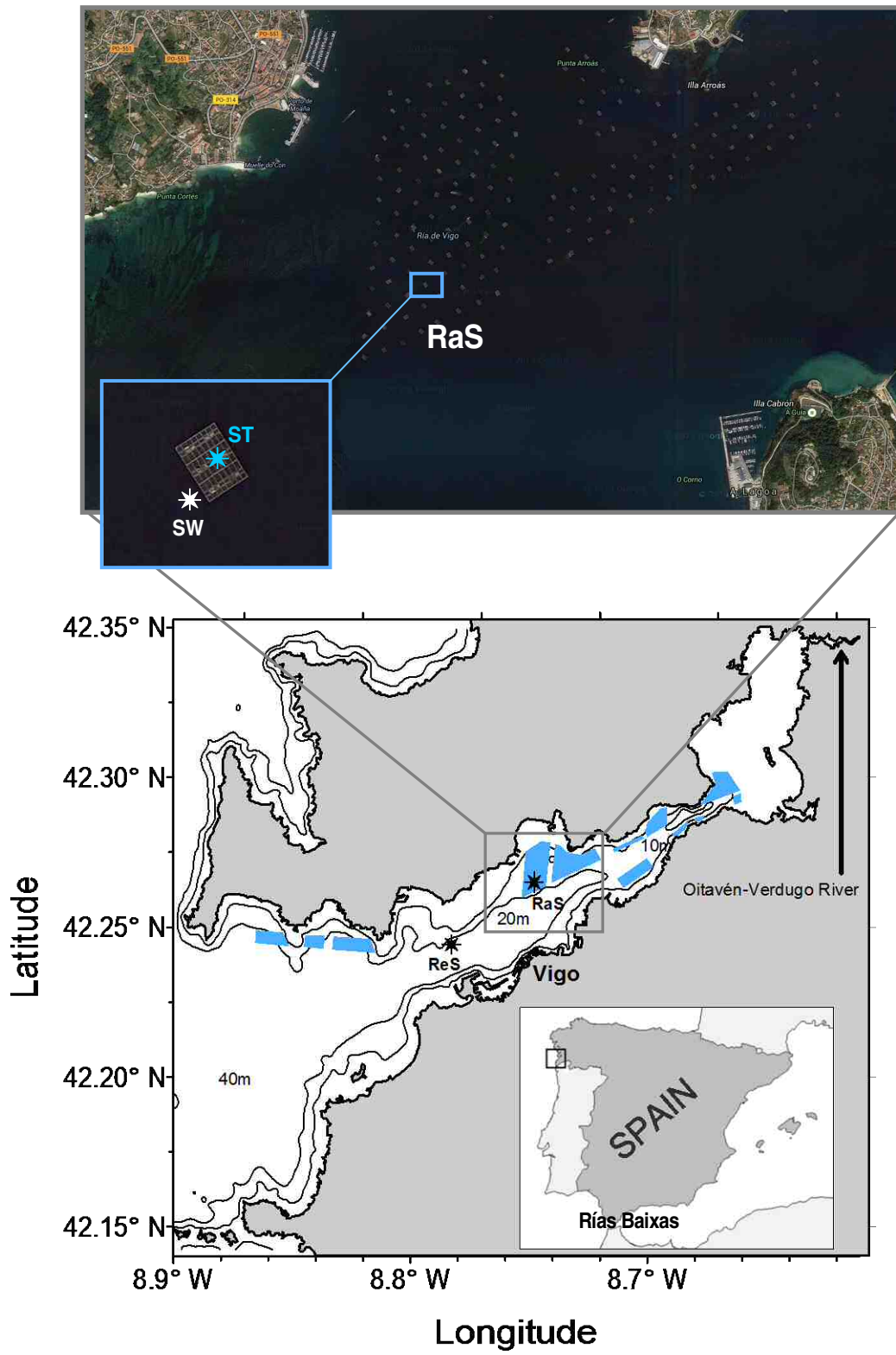


Fig. 1  
Froján et al.

Figure 2

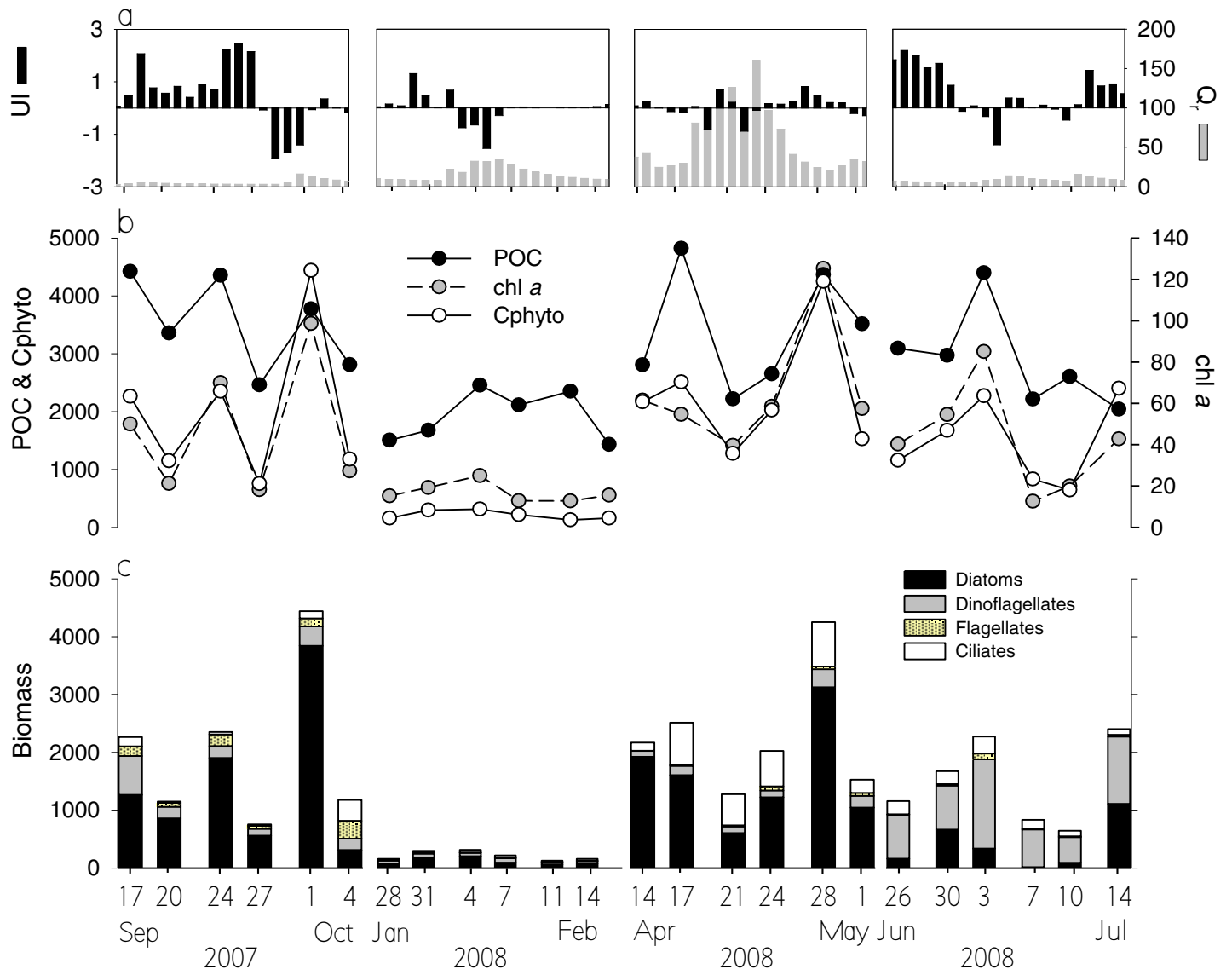


Fig. 2  
Froján et al.

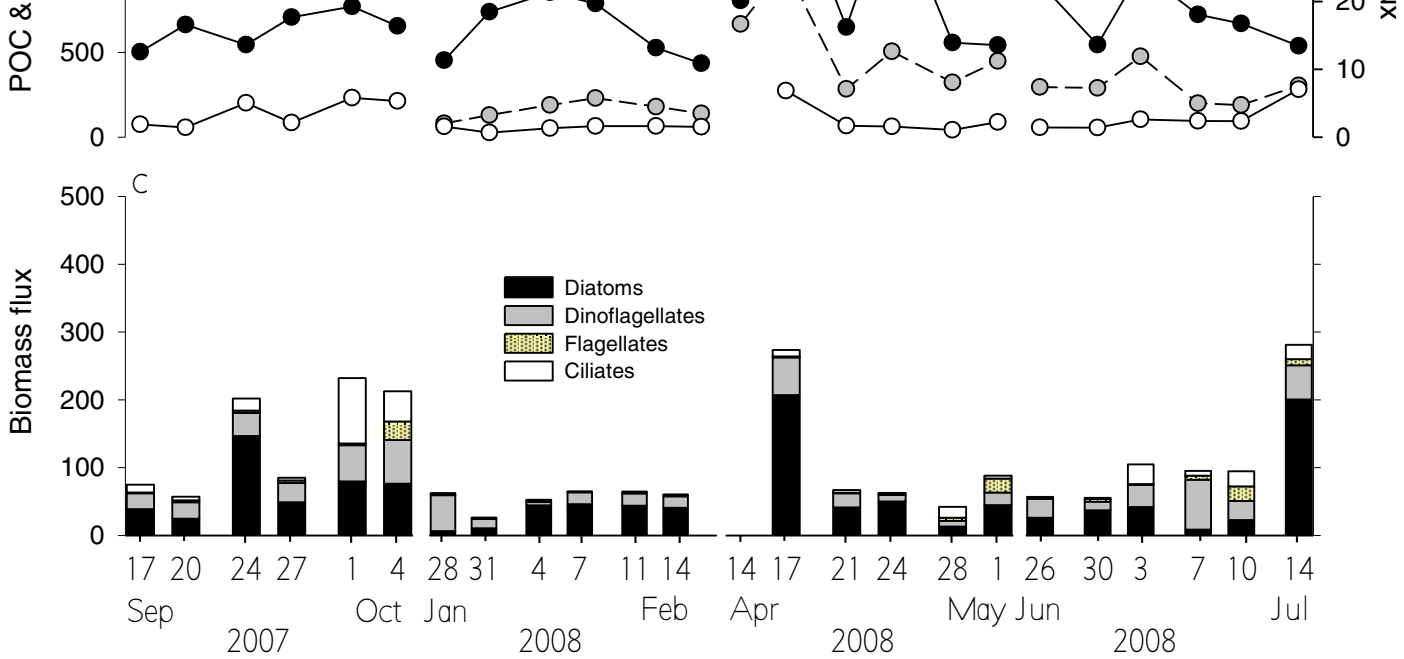


Fig. 3  
Froján et al.



Figure 4

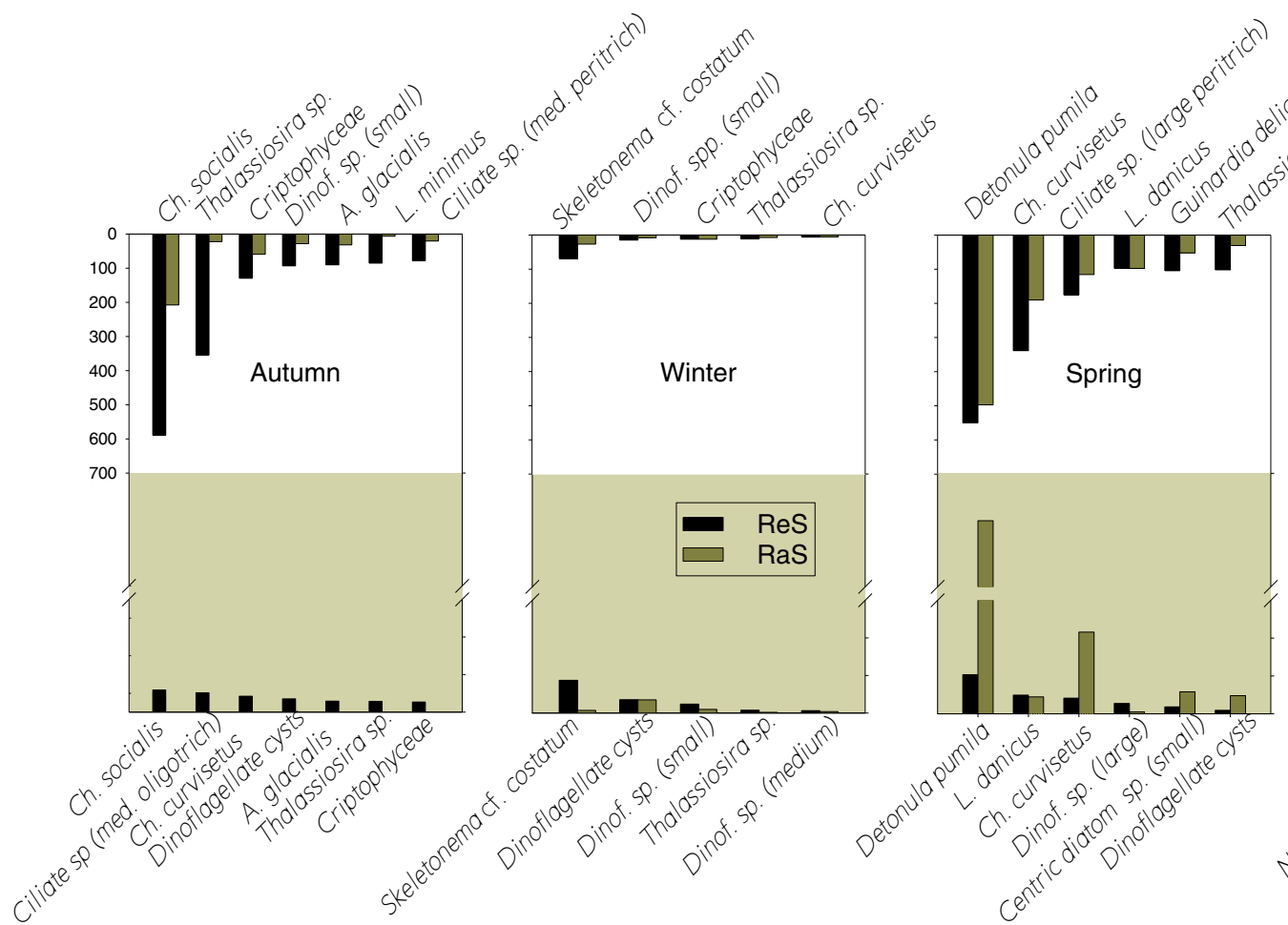


Figure 5

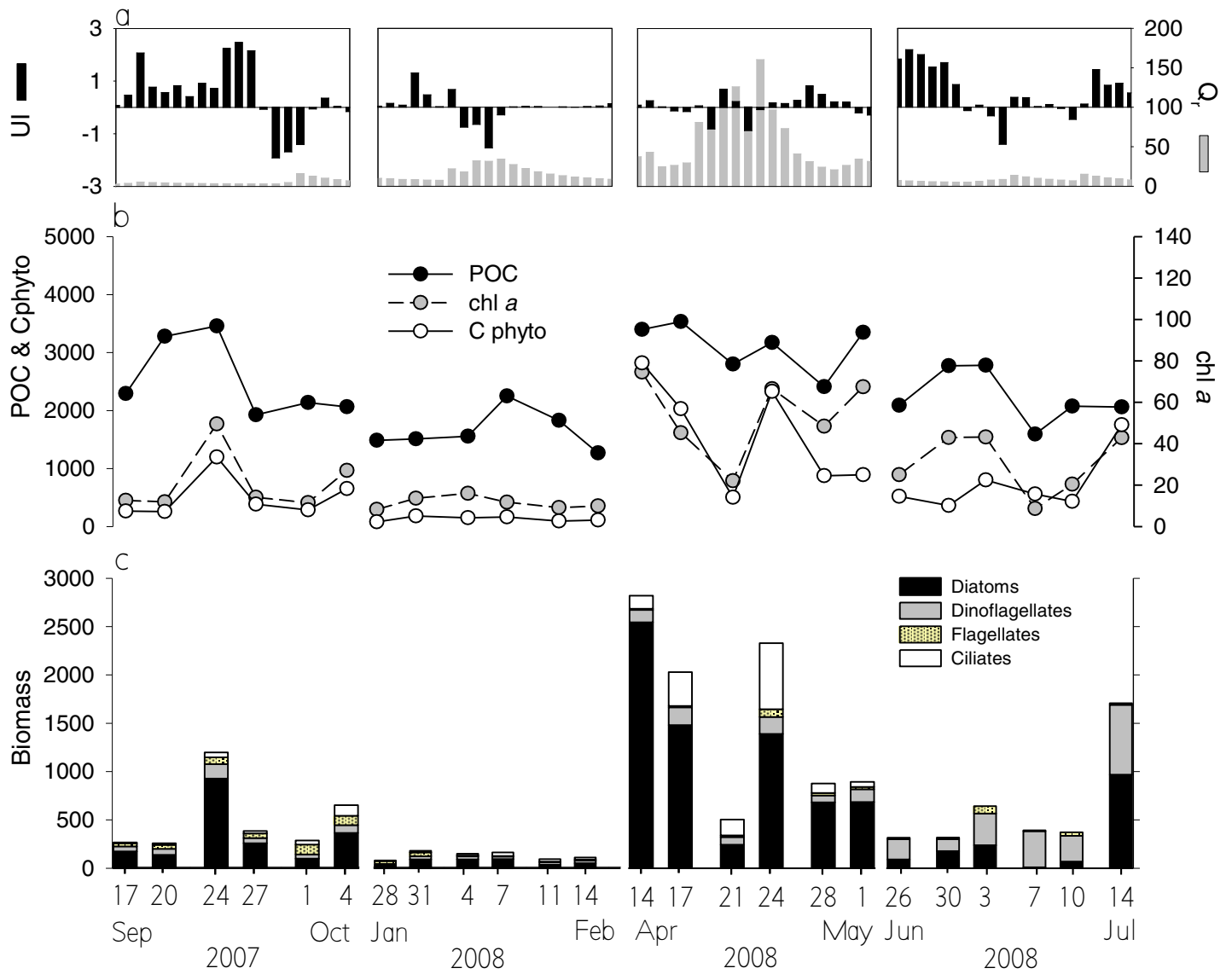


Fig. 5  
Froján et al.

Figure 6

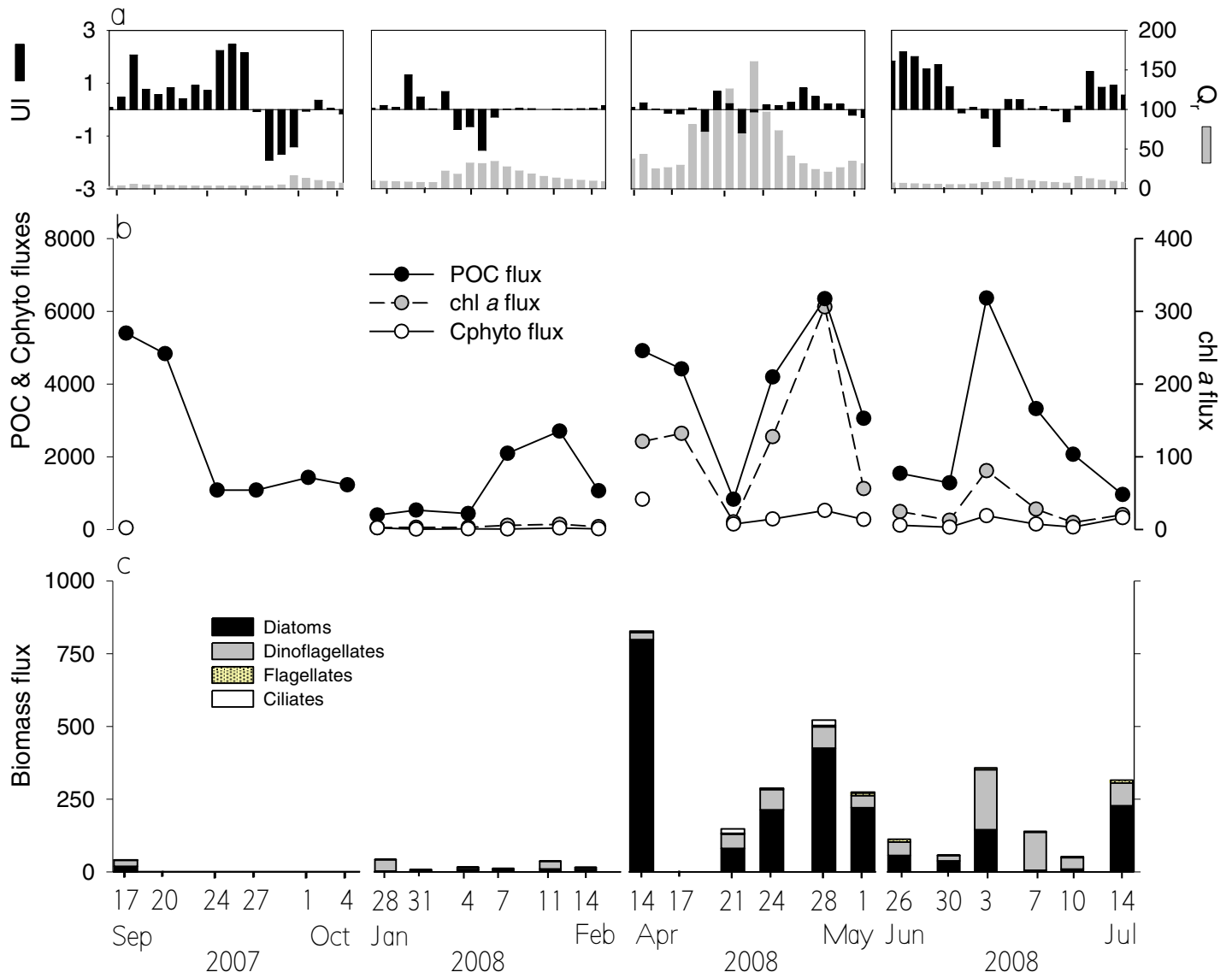


Fig. 6  
Froján et al.

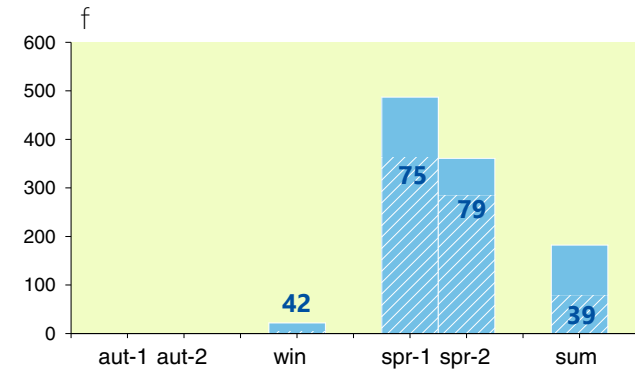
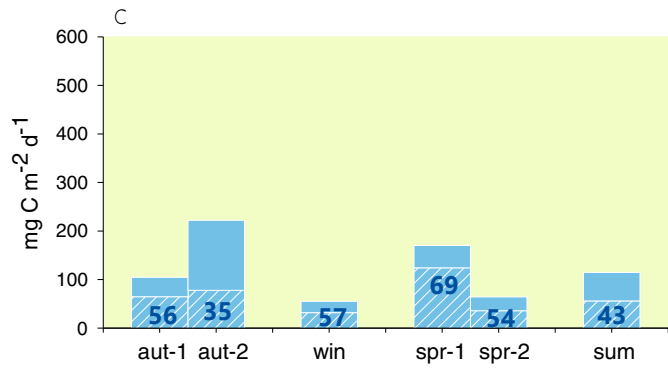
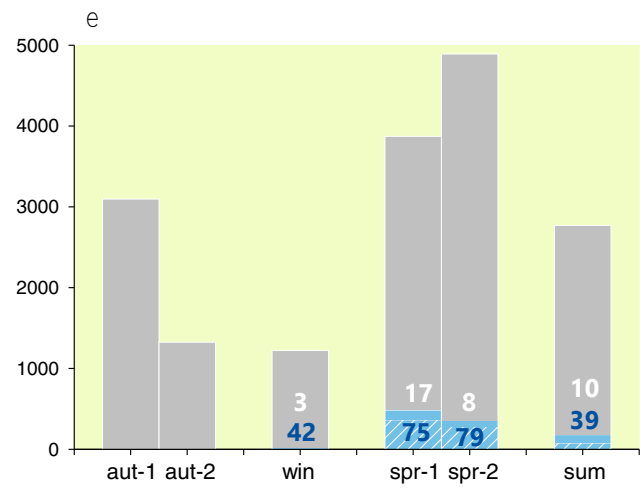
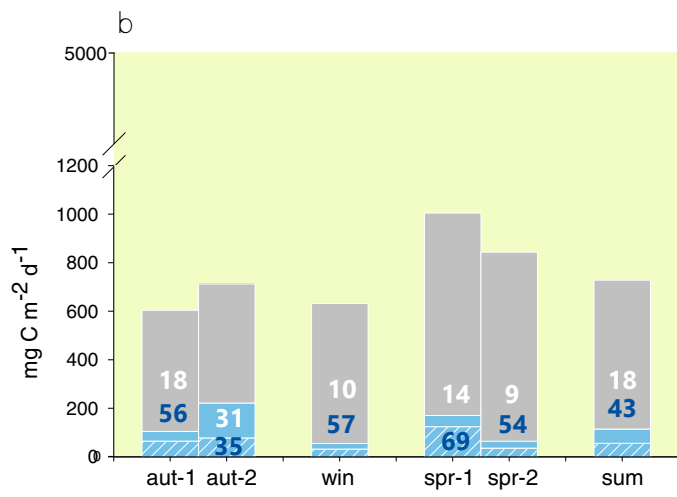


Fig. 7  
Froján et al.

Figure 8

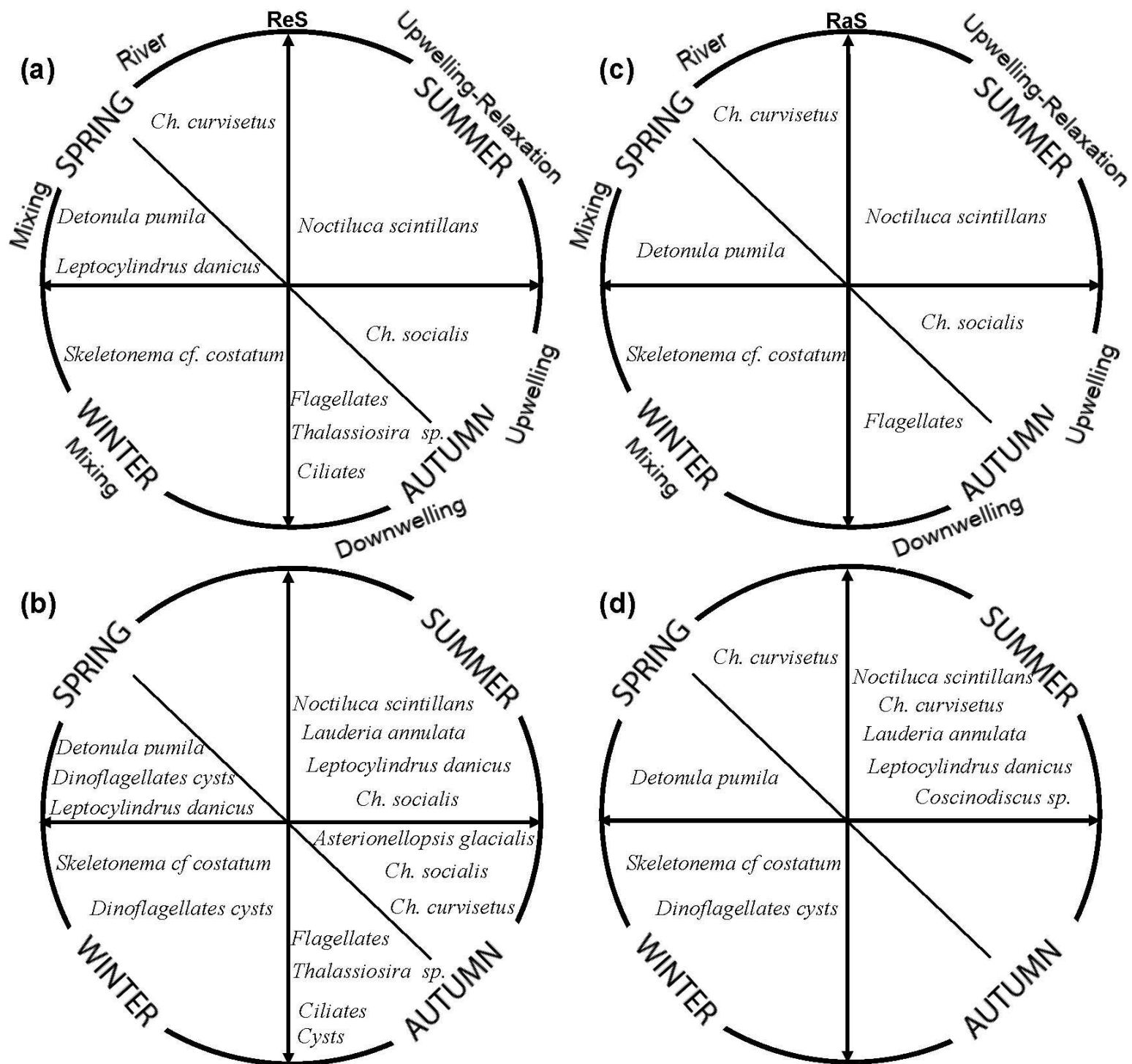


Fig. 8  
 Froján et al.

Table 1

Table 1 Average ( $\pm$  SD) of integrated POC, Cphyto and chl *a* concentrations ( $\text{mg m}^{-2}$ ) in the upper 12 m of the water column, the average ( $\pm$  SD) of integrated Cphyto contribution (%) to integrated POC and the average ( $\pm$  SD) of integrated biomass contribution of diatoms, dinoflagellates, flagellates and ciliates (%) to integrated Cphyto, during each sampling period (autumn, winter, spring and summer) at reference (ReS) and raft (RaS) stations.

	ReS				RaS			
	Autumn	Winter	Spring	Summer	Autumn	Winter	Spring	Summer
<b>POC</b>	3531 $\pm$ 803	1923 $\pm$ 443	3397 $\pm$ 1027	2888 $\pm$ 846	2526 $\pm$ 666	1650 $\pm$ 344	3111 $\pm$ 427	2229 $\pm$ 464
<b>Cphyto</b>	2023 $\pm$ 1348	213 $\pm$ 79	2294 $\pm$ 1057	1498 $\pm$ 740	508 $\pm$ 369	130 $\pm$ 41	1575 $\pm$ 941	739 $\pm$ 520
<b>chl <i>a</i></b>	61 $\pm$ 27	17 $\pm$ 5	66 $\pm$ 30	43 $\pm$ 26	28 $\pm$ 19	11 $\pm$ 3	54 $\pm$ 19	31 $\pm$ 15
<b>% Cphyto:POC</b>	55 $\pm$ 32	11 $\pm$ 4	67 $\pm$ 20	54 $\pm$ 33	20 $\pm$ 11	8 $\pm$ 3	49 $\pm$ 26	35 $\pm$ 26
<b>% Diatoms</b>	66 $\pm$ 22	53 $\pm$ 8	67 $\pm$ 14	22 $\pm$ 17	59 $\pm$ 15	48 $\pm$ 10	71 $\pm$ 15	28 $\pm$ 21
<b>% Dinoflagellates</b>	16 $\pm$ 8	27 $\pm$ 6	8 $\pm$ 3	62 $\pm$ 13	17 $\pm$ 5	22 $\pm$ 4	10 $\pm$ 4	48 $\pm$ 13
<b>% Flagellates</b>	10 $\pm$ 8	7 $\pm$ 4	2 $\pm$ 1	2 $\pm$ 1	16 $\pm$ 10	14 $\pm$ 13	2 $\pm$ 1	5 $\pm$ 4
<b>% Ciliates</b>	8 $\pm$ 11	13 $\pm$ 5	24 $\pm$ 13	14 $\pm$ 6	9 $\pm$ 6	17 $\pm$ 8	17 $\pm$ 12	20 $\pm$ 13

Table 2

Table 2 Average ( $\pm$  SD) POC, Cphyto and chl *a* fluxes ( $\text{mg m}^{-2} \text{d}^{-1}$ ), average ( $\pm$  SD) Cphyto contribution (%) to POC flux and average ( $\pm$  SD) biomass contribution of diatoms, dinoflagellates, flagellates and ciliates (%) to Cphyto flux, during each sampling period (autumn, winter, spring and summer) at reference (ReS) and raft (RaS) stations.

	ReS				RaS			
	Autumn	Winter	Spring	Summer	Autumn	Winter	Spring	Summer
<b>POC flux</b>	640 $\pm$ 100	633 $\pm$ 183	924 $\pm$ 455	728 $\pm$ 185	2507 $\pm$ 2031	1203 $\pm$ 975	3958 $\pm$ 1871	2590 $\pm$ 2026
<b>Cphyto flux</b>	144 $\pm$ 79	55 $\pm$ 15	107 $\pm$ 95	115 $\pm$ 84		22 $\pm$ 14	412 $\pm$ 269	182 $\pm$ 135
<b>chl <i>a</i> flux</b>		4 $\pm$ 1	13 $\pm$ 7	7 $\pm$ 3		4 $\pm$ 2	125 $\pm$ 101	29 $\pm$ 26
<b>% Cphyto:POC</b>	23 $\pm$ 12	10 $\pm$ 4	11 $\pm$ 6	18 $\pm$ 17		3 $\pm$ 4	12 $\pm$ 5	10 $\pm$ 12
<b>% Diatoms</b>	49 $\pm$ 15	57 $\pm$ 27	60 $\pm$ 20	43 $\pm$ 24		42 $\pm$ 22	77 $\pm$ 15	39 $\pm$ 26
<b>% Dinoflagellates</b>	29 $\pm$ 9	38 $\pm$ 27	21 $\pm$ 6	38 $\pm$ 22		54 $\pm$ 23	18 $\pm$ 11	49 $\pm$ 23
<b>% Flagellates</b>	4 $\pm$ 4	3 $\pm$ 3	8 $\pm$ 10	7 $\pm$ 8		4 $\pm$ 5	2 $\pm$ 1	4 $\pm$ 3
<b>% Ciliates</b>	17 $\pm$ 13	2 $\pm$ 2	11 $\pm$ 15	12 $\pm$ 11		1 $\pm$ 1	3 $\pm$ 4	8 $\pm$ 7